Tetrahedron Vol. 38, No. 8, pp. 1035 to 1049, 1982
Printed in Great Britain.

0040-4020/82/081035-15$03.00/0
Pergamon Press Ltd.

ELECTRON TRANSFER ACTIVATION OF THE DIELS–ALDER REACTION

QUANTITATIVE RELATIONSHIP TO CHARGE TRANSFER EXCITED STATES

S. FUKUZUMI and J. K. KOCHI
Department of Chemistry, Indiana University, Bloomington, IN 47405, U.S.A.

(*Received in U.S.A. 4 June* 1981)

Abstract—The Diels–Alder cycloaddition of anthracene to tetracyanoethylene (TCNE) is quantitatively compared to alkylmetal insertion under the same reaction conditions. In both systems, the observation of transient charge transfer (CT) absorption bands is related to the presence of 1:1 electron donor–acceptor complexes of anthracene (Ar) and alkylmetal (RM) donors with the TCNE acceptor. The activation free energies $\Delta G^{\ddagger}$ for anthracene cycloaddition and alkylmetal insertion are found to be equal to the energetics of ion-pair formation, i.e. $[Ar^{+}TCNE^{-}]$ and $[RM^{+}\ TCNE^{-}]$, which are evaluated from the CT transition energies $h\nu_{CT}$. Indeed, the differences in the rates of alkylmetal insertion and anthracene cycloaddition by a factor of more than 10^{9}, are shown quantitatively to arise from the differences in ion-pair solvation ΔG^{s}. The same differences in ΔG^{s} also apply quantitatively to the free ions, $[Ar^{+}]$ and $[RM^{+}]$, independently derived from the electrochemical and iron(III) oxidations of alkylmetals and aromatic compounds, respectively, by outer-sphere electron transfer. The charge transfer formulation of the activation process thus provides a unifying basis for comparing such diverse processes as Diels–Alder cycloadditions and organometal cleavages, when a common electron-deficient acceptor is employed. The relationship to the concerted mechanisms of the Diels–Alder reaction is discussed.

Transient colors were noted in the earliest studies of the Diels–Alder reaction,[1] and ascribed to diene-dienophile complexes, then regarded as intermediates in only the vaguest sense.[2] Andrews and Keefer[3] first paid attention to the color formation, and spectroscopically established the occurrence of 1:1-complexes between arenes and dienophiles such as maleic anhydride and benzoquinone. At about that time, Mulliken[4] formulated the theoretical basis for color formation by what is now well known as the charge transfer (CT) theory. According to Mulliken electron donor-acceptor (EDA) complexes are formed when an electron donor D interacts with an electron acceptor A,

$$D + A \overset{K_{DA}}{\rightleftharpoons} [DA] \tag{1}$$

and the color is associated with the electronic transition from the ground state complex [DA] to the excited ion-pair, i.e.[5]

$$[DA] \xrightarrow{h\nu_{CT}} [D^{+}A^{-}]. \tag{2}$$

Electron donor–acceptor complexes have since been noted, and implicated as intermediates in a number of reactions.[6] For example, in addition to [4+2]-cycloadditions involved in the Diels–Alder reactions, transient colors have been observed in the [2+2]-cycloadditions of electron-rich alkenes such as aryl vinyl sulfides and electron-poor alkenes such as tetracyanoethylene.[7] However, the mechanistic importance of such EDA complexes has been difficult to assess quantitatively. Indeed, little or no attention has been paid to the role of EDA complexes in the majority of the mechanistic studies of either the Diels–Alder reaction[8] or the [2+2]-cycloaddition reactions.[7a,9] The mechanistic involvement of EDA complexes is further obscured by the kinetic dilemma[10] as to whether they are key intermediates along the reaction pathway, i.e.

$$D + A \overset{K_{DA}}{\rightleftharpoons} [DA] \xrightarrow{k_1} \text{adduct} \tag{3}$$

or merely innocent bystanders in an otherwise dead-end equilibrium, i.e.

$$[DA] \overset{K_{DA}^{-1}}{\rightleftharpoons} D + A \xrightarrow{k_2} \text{adduct} \tag{4}$$

As a result, the need to accommodate EDA complexes in mechanistic considerations has generally been ignored.[8,9] Thus, the recent experimental evidence that the Diels–Alder reaction[11] and the related [2+2]-cycloadditions[7e] pass through EDA complexes as in eqn (3), has apparently had little impact on the bulk of the mechanistic output for these synthetically important reactions.[8,9]

The photochemical promotion of cycloaddition reactions, both [4+2]- as well as [2+2]- are known,[12–14] stemming from the classic results on the photochemical cycloaddition of two molecules of maleic anhydride to benzene, which does not otherwise occur thermally.[12] In such photochemical cycloadditions, the EDA complexes play a seminal role in a number of systems.[13] Thus, the addition of maleic anhydride,[13a] as well as maleimide,[13c] to benzene has been shown to proceed via the photoactivation of the EDA complex, rather than the excitation of the individual reactants.[15] Photochemical acceleration of the Diels–Alder reaction of anthracene and maleic anhydride has also been known for some time.[16] The violation of the Woodward–Hoffmann rules[17] for such a [4s+2s]-stereoselective photochemical process has been explained by considering the direct involvement of the CT excited state of the EDA complex.[18]

The foregoing short history points out the dichotomous thoughts regarding the mechanistic importance of EDA complexes in thermal and photochemical cycloadditions. However, there have been few, if

any, studies directed specifically toward the resolution of this issue. Since the focus heretofore has been on only the *ground state* properties of EDA complexes in thermal cycloadditions,[8,9] it is of interest to examine the role of EDA complexes from the viewpoint of their CT *excited states*, which are known to play a crucial role in the photochemical activation of cycloaddition. Indeed, the importance of CT configurations has been emphasized in theoretical treatments of thermal cycloadditions, principally by Epiotis and Shaik.[18,19]

We wish to demonstrate in this study the relevance of the CT excited states of EDA complexes to the activation process for thermal cycloaddition. This approach derives from our earlier analysis of the CT phenomenon as it pertained to the mechanism of alkylmetal insertion with tetracyanoethylene (TCNE).[20] Since TCNE is also a typical dienophile in various Diels–Alder reactions, we believe that the direct comparison of the cycloaddition reaction with TCNE and the insertion reaction with alkylmetals will provide further insight into the general relationship between transition states, attained by thermal, adiabatic processes with charge transfer excited states pumped photochemically.

RESULTS

For the study of the activation process in the Diels–Alder reaction, we have focussed our attention on the interaction of the electron-deficient tetracyanoethylene (TCNE) with various anthracene derivatives. Our approach is to compare this [4+2]-cycloaddition with the interaction of the same polycyanoalkene with a series of organometals leading to insertion, for which the activation process is already known.[20] In both cases, the experimental problem initially centered on the measurement of the CT absorption spectra of the electron donor–acceptor (EDA) complexes of tetracyanoethylene with the anthracenes and with the organometals. The observation of these transient CT spectra was carried out in competition with the thermal reactions of TCNE leading to anthracene cycloaddition and to organometal insertion. The relationship to the charge transfer phenomenon is underscored by the photochemical activation of anthracene cycloaddition and organometal insertion to tetracyanoethylene, under conditions in which the thermal reactions are too slow to compete.

I. *Charge transfer (CT) absorption spectra of anthracenes, alkylmetals and alkenes with tetracyanoethylene*

A. *Anthracenes.* New absorption bands are immediately observed in the visible region upon mixing various anthracenes and related aromatic compounds with tetracyanoethylene in either chloroform or acetonitrile solutions.[6,21] For example, when 10^{-2} M solutions of anthracene and tetracyanoethylene are mixed, a transient blue–green color is observed before the acetonitrile solution becomes colorless in less than a minute. A similar transient color is apparent with 9-bromoanthracene which persists for a slightly longer period, but disappears within a few minutes. The dark green color derived from benz(α)anthracene and TCNE is sufficiently persistent ($\sim$1 hr) to allow the absorption spectrum shown in Fig. 1(a) to be measured. The violet color from naphthalene can be observed for longer than a day. The absorption bands shown in Fig. 1(a) are broad, as are characteristic of intermolecular CT spectra. The absorbance increases with the concentrations of both the aromatic compound (Ar) and TCNE, in accord with absorptions associated with weak 1:1 electron donor-acceptor (EDA) complexes, i.e.[22]

$$\mathrm{Ar} + \mathrm{TCNE} \rightleftharpoons [\mathrm{Ar\,TCNE}]. \qquad (5)$$

The absorption maxima for these EDA complexes correspond to the CT transition energies $h\nu_{CT}$, and they are highly dependent on the structure of the aromatic compounds listed in Table 1. According to Mulliken,[4] the charge transfer interaction is quantitatively given by,

$$h\nu_{CT} = I_D - E_A + \omega \qquad (6)$$

where I_D is the vertical ionization potential of the aromatic donor, and E_A is the vertical electron affinity of the TCNE acceptor. The interaction energy ω is given to first order by the coulombic work term $-e^2/r_{DA}$, in which r_{DA} represents the mean separation of the arene and TCNE in the EDA complex. The direct relationship between $h\nu_{CT}$ and I_D is illustrated in Fig. 2.

The presence of a pair of CT bands in Fig. 1(a) can be ascribed to two transitions, $h\nu^1_{CT}$ and $h\nu^2_{CT}$ corresponding to the excited states $\psi_1(D^+A^-)$ and $\psi_2(D^+A^-)$ of the aromatic donor (D) with the tetracyanoethylene acceptor (A). These excited states can be assigned to transitions from the HOMO and HOMO-1 of the aromatic donor, since the peak separation, $\Delta h\nu_{CT} = h\nu^1_{CT} - h\nu^2_{CT}$, equals the difference ΔI_D between the first and second vertical ionization potentials of the aromatic compound. [For example, the magnitudes of $\Delta h\nu_{CT}$ for benz(α)anthracene (0.53 eV) and naphthalene (0.66 eV) are the same as the values of their ΔI_D of 0.58 and 0.73 eV, respectively.[23]]

B. *Alkylmetals.* New, transient absorption bands are

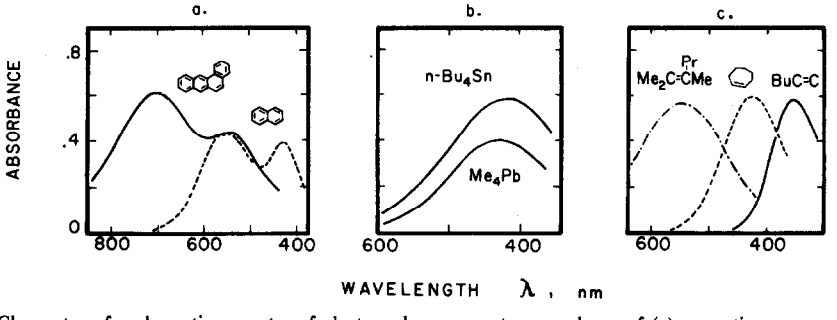

Fig. 1. Charge transfer absorption spectra of electron donor-acceptor complexes of (a) aromatic compounds, (b) alkylmetals and (c) alkenes with tetracyanoethylene. See the Experimental Section for details.

Table 1. Charge transfer spectra of the tetracyanoethylene complexes with aromatic compounds, alkylmetals and alkenes

Aromatic Compound	I_D[a] (eV)	E^{0}[e] (V)	$h\nu_{CT}$ (eV) CH_2Cl_2	CCl_4[h]
anthracene	7.33			1.65[g]
benz(α)anthracene	7.47 (8.05)[b]		1.76 (2.29)	
9-Me-anthracene	7.17	0.79		1.50[g]
2-Me-anthracene			1.60[g]	
9-Et-anthracene	7.19			1.52[g]
9-n-Pr-anthracene				1.53[g]
9-i-Pr-anthracene				1.57[g]
9-t-Bu-anthracene				1.55[g]
9-Br-anthracene	7.38	0.94	1.74	1.74
9,10-Me_2-anthracene	7.04	0.65		1.38[g]
9,10-Br_2-anthracene	7.44	1.02		1.77
naphthalene	8.15 (8.88)[b]		2.24 (2.90)	

Alkylmetal	I_D[c] (eV)	E^{0}[f] (V)	$ClCH_2CHClCH_3$[c]	$CHCl_3$[c]
Me_4Pb	8.90	1.22	3.01	2.90
$EtPbMe_3$	8.65	1.08	2.89	
Et_2PbMe_2	8.45	0.97	2.73	
Et_3PbMe	8.26	0.87	2.59	
Et_4Pb	8.13	0.79	2.52	
Me_4Sn	9.69	1.66	3.76	3.59
$n\text{-}Bu_4Sn$	8.76	1.14	3.15	2.98

Alkene	I_D (eV)	CH_2Cl_2
1-hexene	9.48[d]	3.49
cycloheptene	8.81[d]	2.92
2,3-dimethyl-2-hexene	8.19[d]	2.25

[a] From ref. 23. [b] Value of second I_D. [c] From ref. 20. [d] From Masclet, P.; Grosjean, D.; Mouvier, G.; Dubois, J. J. Electron. Spectrs. 1973, 2, 225. [e] From ref 50. [f] Calcd using Marcus theory, see ref. 42. [g] Value estimated from $h\nu_{CT}$ for chloranil by using: ν(TCNE) = 0.993 ν(chloranil) − 2520 cm^{-1} in ref. 11b. [h] From ref. 11b.

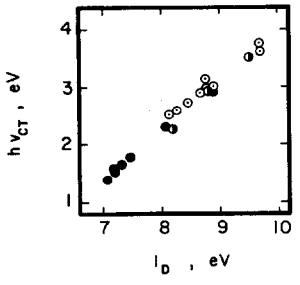

Fig. 2. Correlation of the charge transfer transition energy $h\nu_{CT}$ of TCNE complexes with the first vertical ionization potential I_D of the aromatic compounds ●, alkylmetals ⊙ and the alkenes ◑ listed in Table 1.

also observed in the visible region immediately upon mixing a series of tetraalkyllead and tin compounds with TCNE in either 1,2-dichloropropane or chloroform solutions.[24] The broad absorption bands shown in Fig. 1b due to the EDA complexes of TCNE with tetramethyllead and tetra-n-butyltin, e.g.

$$Me_4Sn + TCNE \rightleftharpoons [Me_4Sn\ TCNE] \qquad (7)$$

are characteristic of all the alkylmetals listed in Table 1. The CT transition energies are highly dependent on the structure of the alkylmetal. Indeed the variation of $h\nu_{CT}$ with the vertical ionization potential of the alkylmetal shows a striking parallel to the linear correlation found for the aromatic compounds in Fig. 2.

The CT absorption bands are all transient, and the rates of their decay depend on the structures of the aromatic compounds and the organometals. The disappearance of the CT band coincides with the formation of the insertion products to be described in the next section.

C. *Alkenes.* The admixture of alkenes with TCNE in acetonitrile solutions also leads immediately to complex formation,

$$\rangle C{=}C\langle + TCNE \rightleftharpoons [\rangle C{=}C\langle\ TCNE] \qquad (8)$$

as shown by the CT absorptions in Fig. 1(c). The absorption maxima indicated by $h\nu_{CT}$ are listed in Table 1, together with those of substituted phenyl vinyl sulfides.[25,26] The correlations of $h\nu_{CT}$ with the ionization potentials of the alkenes are included in Fig. 2.

II. *Kinetics of the thermal activation of electron donor-acceptor complexes*

The appearance of color, which is associated with the formation of the EDA complexes in eqns (5), (7) and (8), is a transient phenomenon. The thermal reactions accompanying the decay of the CT absorbance are individually described below.

A. *Anthracene.* The thermal reaction accompanying the decay of the CT absorption band leads to the Diels–Alder adduct in eqn (9).[11]

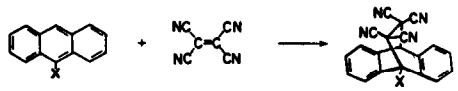

(9)

The rates of the cycloaddition of TCNE to various anthracene derivatives were followed in acetonitrile solutions at 25° by monitoring the disappearance of the anthracene absorbance, as described in detail in the Experimental. The kinetics are expressed by the second order rate expression,

$$\frac{-d[Ar]}{dt} = k[Ar][TCNE] \qquad (10)$$

in accord with previous studies carried out in other solvents.[11] The second order rate constants k were determined either under second order conditions using equimolar amounts of each reactant or under pseudo first order conditions with TCNE in excess, as illustrated in Fig. 3. The rate constants were the same under both conditions (Table 2).

B. *Alkylmetals.* Homoleptic organometals derived from lead, tin and mercury react with TCNE to afford 1:1 adducts which have been characterized as products of TCNE insertion into an alkylmetal bond.[24] For tetramethyltin, the insertion reaction is:

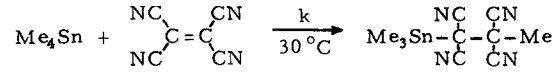

(11)

The rate of the thermal reaction can be monitored spectrophotometrically by following the disappearance of TCNE at 270 nm or the decay of the CT band at 345 nm. The kinetics of the reaction were determined by varying the concentrations, and showed a first order dependence on each reactant by both methods, e.g.[20]

$$\frac{-d[TCNE]}{dt} = k[Me_4Sn][TCNE]. \qquad (12)$$

The second order rate constants k in acetonitrile solutions are listed in Table 2 for a series of alkylmetals.

III. *Photochemical activation of electron donor-acceptor complexes*

In order to demonstrate the direct involvement of the CT interaction in TCNE insertions, the EDA complexes were irradiated under conditions in which the thermal process was too slow to observe. For example, tetramethyltin undergoes no appreciable reaction with TCNE when the acetonitrile solution is cooled to −40°. However, irradiation at this temperature of the CT band at 436 nm (where neither TCNE nor tetramethyltin have significant absorption), leads to the same 1:1 adduct as described for the thermal reaction in eqn (11), i.e.[20]

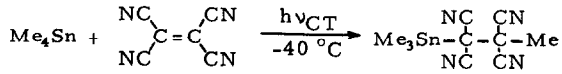

(13)

Insertion induced photochemically at the CT absorption proceeds with unit quantum yield. Furthermore, when an unsymmetrical alkylmetal such as dimethyldiethyltin is employed, the relative amounts of insertion into the methyltin and ethyltin bond are given by the ratio of rate constants, e.g.

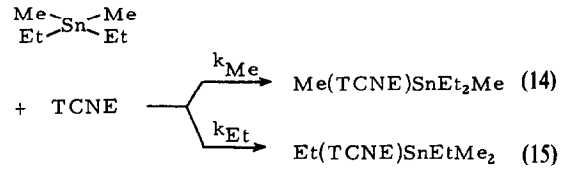

(14)

(15)

The selectivity $S(Et/Me) = k_{Et}/k_{Me}$ is essentially the same in the thermal and photochemical processes, as shown in Table 3.

IV. *Donor properties measured by cyclic voltammetry and chemical oxidation*

The CT interactions described in the foregoing section arise from the aromatic compounds and the organometals acting as electron donors. In order to

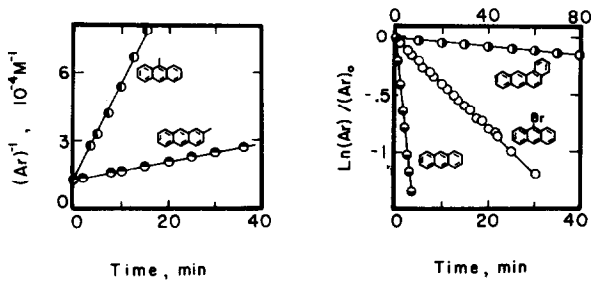

Fig. 3. Kinetics of anthracene cycloaddition to TCNE in acetonitrile solutions at 25°C. (a) Left: second order plot for the formation of TCNE adducts with ● 2-Me-anthracene and ◐ 9-Me-anthracene at 8.60×10^{-5} M. (b) Right: pseudo first order plot using excess (2.15×10^{-3} M) TCNE and ◑ 1.19×10^{-4} M benz(α)anthracene (358 nm), ○ 4.67×10^{-5} M and ○ 9.33×10^{-5} M 9-bromoanthracene (390 nm); ◒ 1.0×10^{-4} M anthracene (376 nm).

Table 2. Second order rate constants for the reactions of TCNE with anthracenes and alkylmetals at 25°

Anthracenes	Second-order Rate Constant, k (M^{-1} s^{-1})			
	CH_3CN		CCl_4[a]	
anthracene	3.3	(0.52)	1.1	(0.04)
benz(α)anthracene	3.1×10^{-2}	(-1.51)		
9-Me-anthracene	1.1×10^{3}	(3.04)	7.3×10^{2}	(2.86)
2-Me-anthracene	3.5	(0.54)		
9-Et-anthracene			3.2×10^{2}	(2.51)
9-Pr-anthracene			2.7×10^{2}	(2.43)
9-i-Pr-anthracene			5.5×10	(1.74)
9-t-Bu-anthracene			9.0×10	(1.95)
9-Br-anthracene	3.1×10^{-1}	(-0.51)	2.2×10^{-1}	(-0.66)
9,10-Me_2-anthracene			4.0×10^{4}	(4.60)

Alkylmetal	CH_3CN[b]	
Me_4Pb	3.2×10^{-2}	(-1.49)
$EtPbMe_3$	5.2×10^{-1}	(-0.28)
Et_2PbMe_2	3.1	(0.49)
Et_3PbMe	1.2×10	(1.08)
Et_4Pb	4.8×10	(1.68)
Me_4Sn	1.5×10^{-5}	(-4.82)
n-Bu_4Sn	9.1×10^{-3}	(-2.04)

[a]Values of 9-bromo- and 9,10-dibromoanthracene from ref. 11b. Others evaluated as in footnote g, Table I. [b]From ref. 20.

Table 3. Selectivity in the thermal and photochemical insertion of alkylmetals with TCNE[a]

Et_nSnMe_{4-n}	Temp. (°C)	Irradiation[b]	S(Et/Me)
Et_2SnMe_2	+22	0	9
	+40	0	10
	-40	436 nm	8
$EtSnMe_3$	+22	0	10[c]
	+40	0	11[c]
	-40	436 nm	9[c]

[a]In acetonitrile solutions from ref. 20. [b]0 is in the dark. [c]Includes the statistical correction.

assess this property quantitatively in solution, we measured their anodic oxidation by cyclic voltammetry and their chemical oxidation by iron(III) complexes.

A. *Cyclic voltammetry.* The cyclic voltammograms (CV) of the various alkylmetals listed in Table 4 were recorded at 25° with a stationary platinum microelectrode in acetonitrile solutions, containing 0.1 M tetraethylammonium perchlorate.[27] The CV of these compounds are all characterized by an anodic wave showing a well-defined current maximum, but no cathodic wave on the reverse scan at sweep rates up to 10 V s^{-1} and temperatures as low as −35°. The details of the sweep dependence of the anodic wave indicate that electron transfer from these alkylmetals is electrochemically unidirectional i.e. totally irreversible.[28] The absence of the reverse electron-transfer step has been shown to derive from the rapid decomposition of the oxidized alkylmetal cation, i.e.

$$Me_4Pb \xrightarrow{-e^-} Me_4Pb^+ \xrightarrow{\text{fast}} Me_3Pb^+ + Me\cdot \qquad (16)$$

Since the initial electron transfer is rate limiting, the anodic peak potential can be shown to be directly related to the activation free energy ΔG‡(E) for heterogenous electron transfer, i.e.

$$\Delta G‡(E) = \beta F E_p + \text{constant} \qquad (17)$$

where F is the Faraday constant and β is the electrochemical transfer coefficient. Indeed the anodic peak potentials E_p correlate linearly with the gas phase ionization potentials I_D of various alkylmetals, as illustrated in Fig. 4(a).

The cyclic voltammetry of the series of substituted benzenes in Table 4 was examined under the same conditions employed for the alkylmetals. The cyclic voltammograms of these aromatic compounds were also characterized by well-defined anodic waves, but no cathodic waves were observed on the reverse scans, even at high scan rates.[29] The irreversible CV behavior suggests that the arene cation formed on anodic oxidation is unstable, in accord with other electrochemical studies.[30]

$$Ar \xrightarrow{-e^-} Ar^+ \xrightarrow{\text{fast}} \text{etc.} \qquad (18)$$

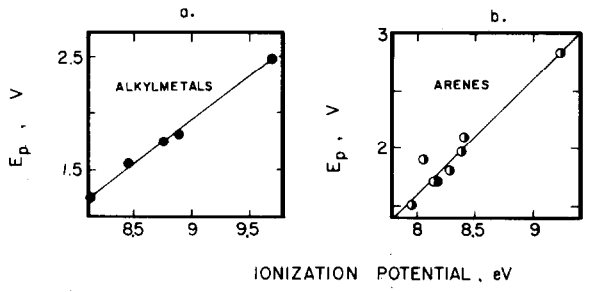

Fig. 4. Linear correlation of the anodic CV peak potential E_p measured at a scan rate of 100 mV s^{-1} in acetonitrile solution with the ionization potentials I_D in the gas phase of (a) left, alkylmetals and (b) right, aromatic compounds.

Table 4. Cyclic voltammetric data for aromatic compounds and alkylmetals in acetonitrile solutions

Aromatic Compound[a]	I_D (eV)	E_p[c] (V)	$E_p-E_{p/2}$ (V)
1,4-$(MeO)_2C_6H_4$	7.96	1.50	0.11
1,3-$(MeO)_2C_6H_4$	8.14	1.70	0.10
1,4-MeO(Me)C_6H_4	8.18	1.71	0.07
1,2-MeO(Me)C_6H_4	8.28	1.80	0.11
$MeOC_6H_5$	8.39	1.96	0.15
1,3,5-$Me_3C_6H_3$	8.40	2.10	0.13
1,2,4,5-$Me_4C_6H_2$	8.05	1.90	0.11
1,2,3,4-$Me_4C_6H_2$		1.89	0.10
C_6H_6	9.23	2.83	0.24
Alkylmetal[b]		d	
Me_4Pb	8.90	1.80	0.18
$EtPbMe_3$	8.65		
Et_2PbMe_2	8.45	1.56	0.18
Et_3PbMe	8.26		
Et_4Pb	8.13	1.26	0.16
Me_4Sn	9.69	2.48	0.14
n-Bu_4Sn	8.76	1.75	0.14

[a] From ref. 33. [b] From ref. 27. [c] In CH_3CN containing 0.1 M $NaClO_4$ at 25 °C at scan rate of 100 mV s^{-1}. [d] In CH_3CN containing 0.1 M Et_4NClO_4 at 25 °C and 20 mV s^{-1}.

Similar to the alkylmetals, Fig. 4(b) shows that the anodic peak potentials measured at constant sweep rates is subject to large and systematic variations which parallel the gas phase ionizations potentials obtained independently from the photoelectron spectra of aromatic compounds.[31]

B. *Chemical oxidation.* Alkylmetals are readily oxidized in acetonitrile solutions by a series of iron(III) complexes,[32]

$$Me_4Sn + FeL_3^{3+} \xrightarrow{k} Me_4Sn^+ + FeL_3^{2+} \qquad (19)$$

where L = various substituted 1,10-phenanthrolines and 2,2'-bipyridine. The reactions obey second order kinetics, being first order in each reactant.

$$-\frac{d[FeL_3^{3+}]}{dt} = k[Me_4Sn][FeL_3^{3+}] \qquad (20)$$

Values of the second order rate constant k for various alkylmetals and iron(III) oxidants are relisted in Table 5 for convenience.

The iron(III) oxidants FeL_3^{3+} also oxidize aromatic compounds,

$$Ar + FeL_3^{3+} \rightarrow Ar^+ + FeL_3^{2+} \qquad (21)$$

by the same overall second order kinetics as those observed in the alkylmetal oxidation, i.e.

$$-\frac{d[FeL_3^{3+}]}{dt} = k[Ar][FeL_3^{3+}] \qquad (22)$$

The second order rate constants k in Table 5 were obtained by spectrophotometrically following the rates of appearance of iron(II) and/or the rates of disappearance of iron(III) under second order and pseudo first order conditions, as illustrated in Fig. 5. The stoichiometric requirement of iron(III) in the oxidation of the aromatic compound was determined by spectral titration of the iron(III). Two equivalents of the iron(III) complexes were reduced for each mole of aromatic com-

Table 5. Kinetic data for the oxidation of aromatic compounds and alkylmetals by iron(III) complexes in $CH_3C^{\cdot}$ at 25°

Aromatic Compound	Second-order Rate Constant, log k (M^{-1} s^{-1})				
	FeL_3^{3+} [a] H	5-Cl	5-NO_2	4,7-Ph_2	bipy
1,4-$(MeO)_2C_6H_4$	-1.80	0.72	2.19	-2.82	-1.80
1,3-$(MeO)_2C_6H_4$	-4.04		1.86		
1,4-MeO(Me)C_6H_4	-3.72	-2.00	-0.37	-4.54	
1,3-MeO(Me)C_6H_4	-5.46	-3.89	-2.40		-5.34
$MeOC_6H_5$	-7.70		-4.36		
1,3,5-$Me_3C_6H_3$	-8.22		-4.47		
1,2,4,5-$Me_4C_6H_2$	-4.09	-2.48	-1.06	-5.42	-4.69
1,2,3,4-$Me_4C_6H_2$	-4.24		-0.37		
RC_6H_5 [b]	b	b	b	b	b
Alkylmetal					
Me_4Pb	1.41	2.22	3.17	0.70	0.96
$EtPbMe_3$	2.59 [c]				
Et_2PbMe_2	3.55	4.44	5.29	2.75	3.15
Et_3PbMe	4.43 [c]				
Et_4Pb	5.03	5.97		4.07	4.50
Me_4Sn	-2.81	-1.76	-0.59	-3.78	-3.29

[a] FeL_3: H = $Fe(phen)_3^{3+}$, 5-Cl = $Fe(5\text{-Cl phen})_3^{3+}$, 5-$NO_2$ = $Fe(5\text{-}NO_2\ phen)_3^{3+}$, 4,7-$Ph_2$ = $Fe(4,7\text{-}Ph_2\ phen)_3^{3+}$, bipy = $Fe(bipy)_3^{3+}$. [b] No reaction for R = Me, Et, n-Pr, n-Bu, i-Pr, t-Bu. [c] Values evaluated from the correlation of log k and I_D in ref. 32.

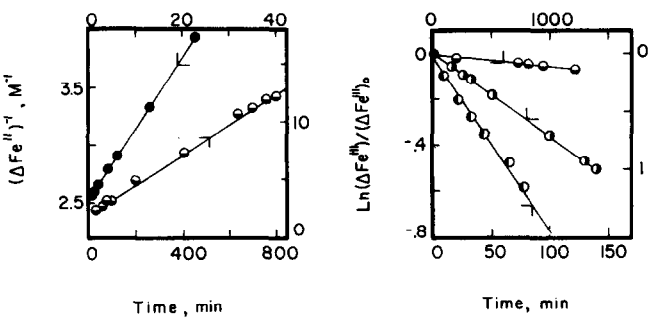

Fig. 5. Kinetics of the oxidation of aromatic compounds by iron(III) oxidants in acetonitrile solutions at 25°. (a) Left: second order plot using equimolar amounts of iron(III) and arene. (b) Right: pseudo first order plots using the arene in excess. See Experimental Section for details.

pound, as described in the Experimental. Accordingly, the values of k in Table 5 are corrected by a factor of 2.

DISCUSSION

Anthracene cycloaddition and alkylmetal insertion with tetracyanoethylene share in common the charge transfer phenomenon shown in Fig. 1 but, at the same time, they represent rather dissimilar reaction types. Thus the Diels–Alder cycloaddition is usually considered to involve a *concerted mechanism* in which the new pair of carbon to carbon bonds are formed simultaneously.[8] On the other hand, the alkylmetal insertion into TCNE is known to involve a *stepwise mechanism*.[20] Thus any mechanistic formulation must reconcile the common observation of charge transfer interactions with the inherent dissimilarities of these processes.

We approach the mechanistic formulation of the Diels–Alder reaction by focussing on the transient charge transfer absorption bands. In particular, we wish to show how the CT formulation provides the unifying concept for anthracene cycloaddition and alkylmetal insertion, by examining the properties of the CT excited states and the unique information provided by the CT transition energies.

I. *Charge transfer formulation for the activation process in the Diels–Alder reaction*

The direct relationship between the Diels–Alder reaction of anthracene with TCNE in eqn (9), and the transient CT absorption is illustrated in Fig. 6, in which the second order rate constant (log k) is plotted against the CT transition energy ($h\nu_{CT}$). The linear correlation spans a range of more than 10^6 in rates, and is expressed as:

$$\log k = -15.4\, h\nu_{CT} + 26 \qquad (23)$$

with a correlation coefficient of 0.99. The same type of linear correlation is also shown in Fig. 6 between the rates of the insertion reaction of alkylmetals with TCNE in eqn (11), and the attendant CT absorption bands,

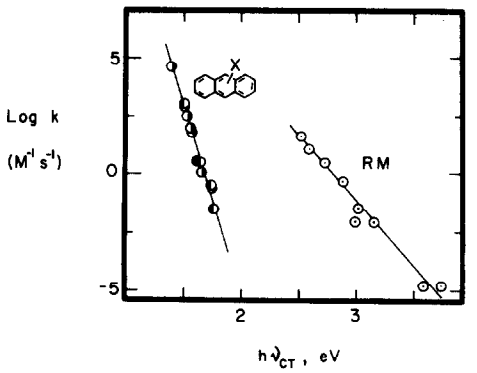

Fig. 6. The correlation of the rates (log k) of TCNE reactions of anthracenes and alkylmetals with the charge transfer transition energies $h\nu_{CT}$ of the EDA complexes.

expressed as:

$$\log k = -5.5\, h\nu_{CT} + 15 \quad (24)$$

with a correlation coefficient of 0.98. The CT interaction of aryl vinyl sulfides and TCNE leading to [2+2]-cycloaddition,[25] can be similarly expressed as:

$$\log k = -11.3\, h\nu_{CT} + 25 \quad (25)$$

with a correlation coefficient of 0.95.

The expression for the anthracenes in eqn (23) merits special attention, since the slope of the correlation is close to unity when the log k and $h\nu_{CT}$ are both expressed in the same units. [For a 1:1 relationship, the equation is log $k = -16.9\, h\nu_{CT} + C$.] In other words, the reactivity of a given anthracene in TCNE cycloaddition, as represented by the activation free energy $\Delta G‡$, is equal to the charge transfer transition energy in the EDA complex, i.e.[33]

$$\Delta G‡ = h\nu_{CT} + \text{constant} \quad (26)$$

We now wish to inquire as to the origin of the striking linear correlations shown in Fig. 6 (and expressed by eqns 23–25), and to discuss how the CT interaction in eqn (26) pertains to the activation process for anthracene cycloadditon.

A. *Nature of the CT excited state and the transition state for anthracene cycloaddition*

For weak EDA complexes of the types described for TCNE in this study, the spectral transition $h\nu_{CT}$ represents an electronic excitation from the neutral ground state to the polar excited state, i.e.

$$[Ar\,TCNE] \xrightarrow{h\nu_{CT}} [Ar^{+}TCNE^{-}]^{*} \quad (27)$$

The asterisk identifies an excited ion-pair with the same mean separation r_{DA} as that in the EDA complex. The nature of the CT excited state has been verified as the polar ion-pair in eqn (27), by applying spectroscopic methods, with pulsed laser excitation.[34] Thus in the EDA complexes of arenes with tetracyanobenzene, the absorption spectrum of the excited complex has been shown to consist of the superposition of the spectral bands of the arene cation Ar^{+} and tetracyanobenzene anion $TCNB^{-}$.[34] Thus the CT transition energy $h\nu_{CT}$ represents the energetics of ion-pair formation, which indeed accords with the generalized Mulliken theory of charge transfer.[4]

Based on the striking correlation in Fig. 6, and expressed in eqn (26), we conclude that the formation of the ion-pair in eqn (27) is tantamount to the activation process in eqn (28) for anthracene cycloaddition to TCNE, i.e.[35]

$$Ar + TCNE \rightarrow [Ar^{+}\,TCNE^{-}]_{s}. \quad (28)$$

Taken further we suggest that the ion-pair $[Ar^{+}\,TCNE^{-}]$ is a reasonable approximation to the transition state for the thermal Diels–Alder process. It should be noted, however, that the transition state is attained by an adiabatic process, whereas the CT excitation represents a vertical (Franck–Condon) transition. As such, the CT excited ion-pair in eqn (27) involves minimal changes in solvation, which occurs only in a subsequent relaxation process, i.e.

$$[Ar^{+}\,TCNE^{-}]^{*} \xrightarrow[\text{solvent}]{\text{fast}} [Ar^{+}\,TCNE^{-}]_{s}. \quad (29)$$

[For example, the relaxation from the Franck–Condon excited state to the equilibrium fluorescent state is associated with an extraordinarily large Stokes shift of 34 kcal mol^{-1} for the toluene-tetracyanobenzene EDA complex in toluene.[36]] By contrast, the formation of the polar ion-pair by a thermal activation must be an adiabatic process which is accompanied by changes in solvation, as indicated by the subscript s in eqn (28). In order to resolve this dilemma, we now evaluate the solvation of aromatic cations since the TCNE moiety is common to all processes.

B. *Solvation of anthracene cations*

Relatively large changes in solvation are expected to accompany formation of the aromatic cation by thermal electron transfer in eqn (28). (The solvation of the neutral complex may be neglected in comparison with that of the ion-pair.[37]) The free energy change for solvation ΔG^{s} is represented by the difference between the gas phase ionization potential, I_D of the arene,

$$Ar \xrightarrow[(gas)]{I_D} Ar^{+} + e^{-} \quad (30)$$

and the free energy change attendant upon its oxidation in solution,

$$Ar \xrightarrow[(solution)]{E^{0}} Ar_{s}^{\cdot+} + e^{-} \quad (31)$$

where the subscript s represents the solvated species. The solvation energies are then evaluated quantitatively by the relationship:[38]

$$\Delta G^{s} = I_D - FE^{0} - FC \quad (32)$$

where ΔG^{s} is the free energy change in solvation relative to the neutral arene, E^{0} is the standard oxidation potential listed in Table 6, C is a constant (4.40 V for SCE),[40] which includes the potential of the reference electrode on the absolute scale together with the liquid junction potentials, and F is the Faraday constant. The values of

Table 6. Solvation energies of anthracene and alkylmetal cations in acetonitrile

Anthracene	I_D (eV)[a]	E^0 (V vs SCE)[b]	$-\Delta G^s$ (eV)[c]
9-methyl	7.17	0.79	1.98
9-bromo	7.38	0.94	2.04
9,10-dimethyl	7.04	0.65	1.99
9,10-dibromo	7.44	1.02	2.02
Alkylmetal			
Me_4Pb	8.90	1.22	3.28
$EtPbMe_3$	8.65	1.08	3.17
Et_2PbMe_2	8.45	0.97	3.08
Et_3PbMe	8.26	0.87	2.99
Et_4Pb	8.13	0.79	2.94

[a]From refs. 25 and 24. [b]From ref. 50. [c]Calculated from eq 32.

the solvation energies of the anthracene cations obtained in this manner in Table 6, are remarkably invariant at 2.01 ± 0.03 eV. As such, it is simply included as an additive term for the constant in eqn (26). The constancy of the solvation term thus underscores the essential equivalence of the $[Ar^+ TCNE^-]$ ion-pair generated for the CT excited state in eqn (27) with that developed for the transition state in eqn (28).

II. *Charge transfer formulation of alkylmetal insertion*

The linear correlation shown on the right side of Fig. 6 accords with the CT mechanism previously developed for alkylmetal insertion with TCNE,[20] as summarized below.

$$RM + TCNE \rightleftharpoons [RM\ TCNE] \tag{33}$$

$$[RM\ TCNE] \xrightarrow{k} [RM^+\ TCNE^-]_s \tag{34}$$

$$[RM^+\ TCNE^-]_s \xrightarrow{\text{fast}} R(TCNE)M \tag{35}$$

Scheme 1.

where RM represents the various alkylmetals. It is important to emphasize that the rate-limiting electron transfer step in Scheme 1, eqn (34), can be independently demonstrated by showing that the deliberate photochemical pumping of the CT excited state at $-40°$, i.e.

$$[RM\ TCNE] \xrightarrow[-40°C]{h\nu CT} [RM^+\ TCNE^-]^* \tag{36}$$

$$[RM^+\ TCNE^-]^* \xrightarrow{\text{fast}} [RM^+\ TCNE^-]_s, \text{ etc.} \tag{37}$$

Scheme 2.

leads to alkylmetal insertion with the same selectivity in eqns (14) and (15), as that obtained from the thermal reaction (Table 3). Thus common intermediates must be involved in the thermal and photochemical processes, in accord with Schemes 1 and 2, respectively.

Solvation energies of the alkylmetal cations must again relate the adiabatic ion-pair in eqn (34) with the vertical (Franck–Condon) ion-pair in eqn (36), as described above for the anthracenes. However, the solvation energies of the alkylmetal cations in Table 6 differ in two ways from those of the anthracene cations. First, the solvation energies of the alkylmetal cations are more than 20 kcal mol^{-1} larger than those of the anthracene cations. Second, the solvation energies of alkylmetal cations are not constant, but decrease with increasing size of the alkyl ligands. Both of these differences are important factors which quantitatively interrelate anthracene cycloaddition with alkylmetal insertion, as described in the following section.

II. *Quantitative comparison of anthracene cycloaddition and alkylmetal insertion with TCNE as the common electron acceptor*

An important test of the CT formulation for anthracene cycloaddition in eqn (9) would be provided by demonstrating its interrelationship with the alkylmetal insertion in eqn (11), particularly since the rates in Table 2 differ by a factor of more than 10^9. If the CT activation of the Diels–Alder reaction is valid, it must also relate directly to the activation process for alkylmetal insertion of TCNE, for which the CT interactions have been already established.[20] Such an interrelationship must be made in the teeth of the apparent diversity of the two processes shown in Fig. 6, in which the linear free energy relationship for anthracene cycloaddition differs from that for alkylmetal insertion in two important ways. First, the correlation of the alkylmetals is displaced by about 1 eV to higher energies relative to the anthracene correlation. Second, the slope of the alkylmetal correlation is quite different from the slope of the anthracene correlation, being smaller by a factor of more than 2.

The correlations in Fig. 6 do not specifically include solvation changes. It is clear, however, that solvation must be taken into account, since values of ΔG^s in the two processes differ in significant ways. For example, ΔG^s for the various anthracene cations is rather invariant with structure, whereas ΔG^s for the alkylmetal cations are not only structure dependent, but quite a bit larger as well (Table 6). *If the change in solvation is included in the correlation, the two separate lines in Fig. 6 are remarkably merged into a single line, shown in Fig. 7.* Thus the activation processes for anthracene cycloaddition and alkylmetal insertion of TCNE are both des-

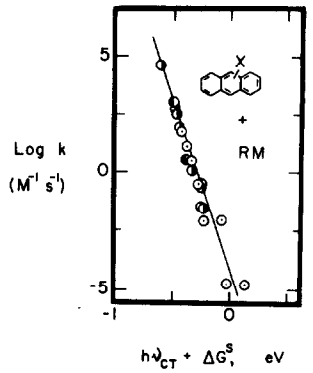

Fig. 7. Unified correlation of the activation free energies for anthracene cycloaddition and alkylmetal insertion with TCNE, according to the charge transfer formulation in eqn (38). Compare with Figure 6.

cribed by a single, common relationship expressed as:

$$\Delta G‡ = h\nu_{CT} + \Delta G^s + \text{constant.} \quad (38)$$

According to eqn (38), the higher reactivity of alkylmetals relative to anthracenes derive from the larger changes in solvation during the activation process. Otherwise, there is no intrinsic difference in the activation barrier between anthracene cycloaddition and alkylmetal insertion with tetracyanoethylene. The interrelationships among the EDA complex, the CT excited state and the transition state is illustrated in the thermochemical cycle below:[35]

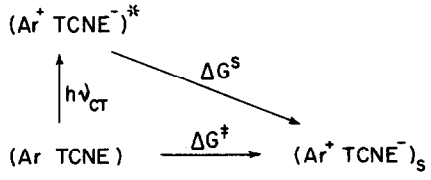

Scheme 3.

It is important to emphasize that the CT formulation as expressed in eqn (38) does not depend on resolving the question, initially posed in eqns (3) and (4), to prove whether the EDA complex is or is not along the reaction coordinate.[41]

The absence of data for I_D and E^0 of the olefins listed in Table 1, unfortunately does not as yet permit us to test the general applicability of eqn (38) to the [2+2]-cycloaddition of olefins with TCNE.[7] However, the successful merging of the anthracene cycloaddition with the alkylmetal insertion augurs well for such an extension to [2+2]-cycloadditions, particularly since the linear correlation of the alkene cycloaddition[25] lies *between* the correlations of the anthracene cycloaddition and the alkylmetal insertion.

III. *Quantitative comparison of the formation of aromatic and alkylmetal cations in solution*

The activation processes for anthracene cycloaddition and alkylmetal insertion with TCNE, as schematically described in eqns (28) and (34), respectively, are representative of an inner-sphere mechanism for electron transfer.[42] As such, the interaction energy ω of the ion-pairs, $[Ar^+ TCNE^-]$ and $[RM^+ TCNE^-]$, which is evaluated as the coulombic work term, makes an important contribution to the activation barrier. At this juncture, the question arises as to the nature of such ion-pairs, particularly with regard to the full development of charge and the structural integrity of the component donor cation. (Note the TCNE counter anion is common to both processes.)

In order to address this question, we now direct our attention to the chemical oxidation of alkymetals and aromatic compounds by the series of outer-sphere iron(III) oxidants,[43] FeL_3^{3+} with L = substituted 1,10-phenanthroline ligands, as described in eqns 19 and 21, respectively. The second order rate constants (log k′) of such outer-sphere electron transfers provide a means of directly comparing the energetics associated with the formation of aromatic cations, i.e.

$$Ar \xrightarrow[CH_3CN]{k'} Ar_s^+ + [e^-] \quad (39)$$

with those of alkylmetal cations,

$$RM \xrightarrow[CH_3CN]{k'} RM_s^+ + [e^-] \quad (40)$$

where both are formed rather free from strong counterion influences.

In Fig. 8(a), the rate constants (log k′) for the oxidations with $Fe(phen)_3^{3+}$ is plotted against the ionization potentials of the alkylmetal and the aromatic compounds listed in Table 5. The linear correlations correspond to the relationship:

$$\log k' = \alpha I_D + \text{constant} \quad (41)$$

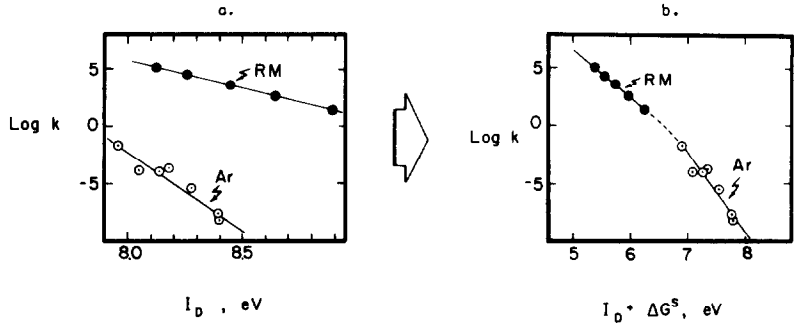

Fig. 8. Correlation of the rates (log k′) of the outer-sphere oxidation with $Fe(phen)_3^{3+}$ and the vertical ionization potentials I_D of alkylmetals (RM) and aromatic compounds: (a) before and (b) after inclusion of cation solvation.

where $\alpha = -16.9$ and -4.9 for the aromatic compounds and the alkylmetals, respectively. It is important to note that in these outer-sphere oxidations, the reactivity of a given alkylmetal is clearly more than 10^9 times greater than the reactivity of an aromatic compound with the same value of I_D. However, if the difference in *cation solvation is taken into account, the reactivity of aromatic compounds follows the same trend as the alkylmetals*, as shown in Fig. 8(b). The resulting unity of alkylmetals and aromatic compounds in outer-sphere electron transfer can be expressed in terms of a single linear free energy relationship based on Marcus theory, as described further in the Experimental. At this point, however, we wish to emphasize that the dramatic effect of cation solvation in merging the outer-sphere oxidation of aromatic compounds and alkylmetals in Fig. 8(b) is exactly the same as that employed in the merging of the ion-pairs in the inner-sphere mechanism in Fig. 7. Indeed, such an equality provides strong support for the CT formulation of the ion-pairs $[Ar^+ TCNE^-]$ and $[RM^+ TCNE^-]$ as transition state models in anthracene cycloaddition and alkylmetal insertion with tetracyanoethylene.

IV. *Comments on the CT formulation and the concerted Diels–Alder reaction*

In this study, we have shown that the activation process for alkylmetal insertion and anthracene cycloaddition are the same. However, the stepwise mechanism in Scheme 1, previously demonstrated for alkylmetal insertion,[20] contrasts with the concerted mechanism typically considered for the Diels–Alder reaction.[8] How then is CT activation related to a concerted process? Epiotis has provided a useful basis on which to discuss this question.[19,44] In his theoretical treatment of pericyclic reactions, the importance of configuration interaction in determining the properties of the transition states has been established in various types of thermal and photochemical pericyclic reactions, including the Diels–Alder reaction. For the polar type of Diels–Alder reaction examined in this study,[45] the most important configuration in the transition state according to Epiotis is the CT configuration, i.e. $[D^+A^-]$. Recently, Shaik[46] has expanded on this theory to include more general cases which involve covalent bond-making and bond-breaking steps between donors and acceptors. In this formulation, the closed-shell reactants D and A are prepared for bonding by promotion to open-shell entities via the charge transfer configuration, since it contains the "image" of the product, i.e.[47]

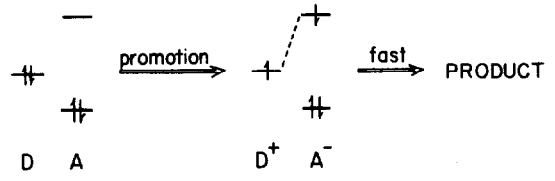

Scheme 4.[46]

The distinction between concerted and stepwise mechanisms may be based on Scheme 4 by the degree of the HOMO–LUMO interaction. For example, the HOMO–LUMO interaction for alkylmetal–TCNE insertion is symmetry-forbidden owing to the antisymmetric LUMO of TCNE and the symmetric HOMO of the alkylmetals.[48] A stepwise process may thus be expected, in contrast to the symmetry-allowed HOMO–LUMO interaction for the anthracene–TCNE cycloaddition.[8,45] The HOMO–LUMO interactions in the oxidation of alkylmetals and aromatic compounds by an outer-sphere electron transfer mechanism must, by definition,[49] involve limited HOMO–LUMO interactions. One can conceive, thus, of a spectrum of electron transfer activation processes from the limits of the outer-sphere mechanism to various concerted processes, such as the Diels–Alder reaction, at the other extreme.

The experimental criteria for concerted mechanisms have generally depended on (1) the observation of stereospecificity and (2) the effect of polar solvents on the rates.[8] However, their application is not without some ambiguity. For example, the tight ion-pairs such as those presented in this study could collapse stereospecifically. Furthermore, the solvation energies ΔG^s of reactive cations are, by and large, undetermined, and lend uncertainty as to the solvent effect which may be anticipated. Thus the recent measurements of the solvation energies of anthracene and related ions,[50] have led to the unexpected result that ΔG^s is rather invariant in solvents as structurally diverse as dioxane, acetonitrile and dimethylformamide. Clearly, more definitive, quantitative studies of solvation are required.

SUMMARY AND CONCLUSIONS

The transient colors observed during the Diels–Alder reaction of various anthracenes and tetracyanoethylene arise from electron donor-acceptor complexes, which are analogous to the intermediates in the insertion of alkylmetals into TCNE. The CT transition energies $h\nu_{CT}$ in these systems are proportional to the vertical ionization potentials of the aromatic compound (Ar) and the alkylmetal (RM), in accord with the Mulliken theory of CT. The rates of alkylmetal insertion are generally more than a factor of 10^9 faster than anthracene cycloaddition for donors which have comparable ionization potentials. Nonetheless, the second order rate constants (log k) for anthracene cycloaddition and alkylmetal insertion with TCNE are both linearly related to the CT transition energies, on the two separate correlations. The magnitude of the slope indicates that activation barrier for anthracene cycloaddition is the same as the CT transition energy to the excited ion-pair state of the EDA complex. Equating the transition states to the CT excited ion-pairs $[Ar^+ TCNE^-]$ and $[RM^+ TCNE^-]$ for cycloaddition and insertion, respectively, requires knowledge of the solvation change attendant upon ion-pair formation. Indeed the inclusion of solvation (evaluated independently from the gas phase ionization potential I_D and the standard oxidation potential E^0 in solution) leads to a *single* linear free energy correlation of the activation barrier $\Delta G^{\ddagger}$ and the CT excited state $h\nu_{CT}$. Therefore, eqn (38) is simultaneously applicable to such diverse processes as anthracene cycloaddition and alkylmetal insertion. We conclude that the large reactivity difference between alkylmetal insertion and anthracene cycloaddition with TCNE is made up almost entirely by differences in ion-pair solvation.

The importance of solvation changes is also underscored in a related comparison of the one-electron oxidation of a series of aromatic compounds and alkylmetals by outer-sphere electron transfer as they are effected heterogeneously at an electrode surface or homogeneously by a graded series of iron(III) oxidants.

The alkylmetals undergo outer-sphere electron transfer at rates which are at least 10^9 times faster than aromatic compounds of comparable ionization potentials. When solvation energies of the cations [RM^+] and [Ar^+] are explicitly taken into account, however, the activation free energies fall on a single correlation with the standard oxidation potential of the arene or the alkylmetal. This unified correlation abides by the Marcus theory of outer-sphere electron transfer. The equivalence of solvation differences between the ion-pairs [Ar^+ $TCNE^-$] and [RM^+ $TCNE^-$] compared to those in the free ions [Ar^+] and [RM^+], represents additional strong support for the charge transfer formulation of the Diels–Alder reaction, especially the polar or normal types.

EXPERIMENTAL

Materials. Fe(II) complexes were prepared by adding an equiv. amount of the appropriate ligand to an aqueous soln of $FeSO_4$. 1,10-Phenanthroline (monohydrate) and 2,2′-bipyridine were obtained from Fisher Scientific Co. and J. T. Baker Chemical Co., respectively. The substituted 1,10-phenanthroline ligands were obtained from G. F. Smith Chemical Co. The salts of the Fe(II) complexes were prepared as the hexafluorophosphate or perchlorate. The Fe(III) complexes were prepared by ceric oxidation of an acidic aqueous soln of the corresponding Fe(II) complexes.[32] After complete oxidation, ammonium hexafluorophosphate or sodium perchlorate was added to precipitate the Fe(III) salts. The Fe(III) complex of 5-nitro-1,10-phenanthroline was generated *in situ* by electrolytic oxidation of the corresponding Fe(II) complex in acetonitrile, using 0.1 M tetraethylammonium perchlorate as the supporting electrolyte.

The aromatic compounds used in this study were described previously.[35] Since the rates were sensitive to olefinic impurities care was taken for the purification of the aromatic compounds, especially the less reactive ones such as mesitylene, in which oxidation is quite slow. Thus, mesitylene was initially sulphonated by dissolving it in concentrated H_2SO_4. Mesitylene sulphonic acid was precipitated by the addition of concentrated HCl at 0°, washed with cold conc HCl, and recrystallized from $CHCl_3$. The sulfonic acid was hydrolyzed by boiling it in 20% HClaq, and the separated mesitylene was dried over $CaCl_2$, and distilled from Na. Acetonitrile used as a solvent was reagent grade material obtained commercially. It was further purified by stirring with calcium hydride overnight. After filtration, the acetonitrile was treated with $KMnO_4$ and redistilled from P_2O_5 under a N_2 atmosphere.

Spectral measurements of the CT absorption bands. The CT spectra in Fig. 1 and the transition energies in Table 1 were measured by the procedures described previously.[20] The spectra in Fig. 1 were obtained under the following experimental conditions: (a) At 25°, 1.87×10^{-2} M TCNE in CH_2Cl_2 with 1.46×10^{-2} M benz(α)anthracene and 2.60×10^{-2} M naphthalene (dashed line). (b) At −10°, 0.46 M n-Bu_4Sn and 1.5×10^{-2} M TCNE, and 0.30 M Me_4Pb and 1.0×10^{-2} M Me_4Pb in $CHCl_3$ from Ref. 24. (c) At 25°, 1.87×10^{-2} M TCNE in CH_2Cl_2 with 0.33 M 1-hexene, 0.34 M cycloheptene and 0.40 M 2,3-dimethyl-2-hexene.

Kinetics of the Diels–Alder reaction. The rates in acetonitrile were measured spectrophotometrically on a Cary 14 Spectrophotometer at 25°, by monitoring the decrease in absorbance of anthracene. The wavelengths used for the analysis varied for the different arenes as follows: anthracene, 376 nm; 9-methylanthracene, 386 nm; 2-methylanthracene, 378 nm; 9-bromoanthracene, 390 nm; benz(α)anthracene, 358 nm. For reactive compounds such as 9-methylanthracene and 2-methylanthracene, the rates were followed under second order conditions using equiv. concentrations (8.60×10^{-5} M) of the anthracene and TCNE. The second order rate constants k were determined from the relationship: $[Ar]^{-1} = [Ar]_0^{-1} + 2kt$, where $[Ar]_0$ and [Ar] are the concentration of the anthracene at time = 0 and time = t. [Fig. 2a.] For the less reactive compounds such as benz(α)anthracene, anthracene, and 9-bromoanthracene, the rates were followed under pseudo first order conditions using excess TCNE(2.15×10^{-3} M). The second order rate constants were determined from the pseudo first order rate constants obtained from the slopes in Fig. 2(b), according to the relationship: $\ln[Ar]_0/[Ar] = -k[TCNE]_0t$.

Kinetics of arene oxidation. The rates of the oxidation of aromatic compounds were followed spectrophotometrically at 25° in acetonitrile solns, either by the appearance of the Fe(II) bands or the disappearance of the Fe(III) bands. The spectroscopic data for the Fe(II) and Fe(III) complexes were described previously.[32] Solns of the Fe(III) complexes (4.3×10^{-4} M ~ 1.0×10^{-2} M) were freshly prepared in acetonitrile under argon. A Schlenk flask equipped with a small side arm fused to a square quartz cuvette (3 mm or 10 mm I.D.) was used for the kinetic measurements. A 1.0 mL (or 3 mL for a 10 mm I.D. cell) aliquot of a stock Fe(III) soln was introduced with a glass pipette, and an appropriate amount of an aromatic compound was transferred to the side arm under argon. The Schlenk cell was placed in the thermostatted compartment (at 25°) of the spectrophotometer. After thermal equilibration (~ 5 min), the two components were mixed by vigorously shaking the Schlenk cell for a few secs, and the spectrum was recorded immediately.

The kinetics were followed either by the appearance of the Fe(II) bands or the disappearance of the Fe(III) bands. With equivalent stoichiometric amounts of each reactant (i.e. $[Fe^{III}] = 2[Ar]$), the rate of the appearance of Fe(II) is given by: $\{[Fe^{II}]_\infty - [Fe^{II}]\}^{-1} = 2kt + [Fe^{II}]_\infty^{-1}$, as shown in Fig. 5(a). The equivalent expression was applied to the disappearance of Fe(III). For example with excess arene, it is: $\ln\{[Fe^{III}] - [Fe^{III}]_\infty\}/\{[Fe^{III}]_0 - [Fe^{III}]_\infty\} = -2\ k[Ar]_0t$ and with excess iron(III): $\ln\{[Fe^{III}]/[Fe^{III}]_0\} = -k[Fe^{III}]_0t$. Both of these rate expressions agree in Fig. 5(b) with the overall second order kinetics, being first order in each reactant, in accord with eqn (22). The experimental conditions in Fig. 5 are: (a) Left: second order plot for the formation of Fe(II) from 4.2×10^{-4} M $Fe(Cl\ phen)_3^{3+}$ and ● 2.1×10^{-4} M *p*-dimethoxybenzene and ◒ 4.4×10^{-4} M *p*-methylanisole. (b) Right: pseudo first order plot for the consumption of Fe(III) with ◒ 1.6×10^{-2} M *p*-methylanisole and 4.0×10^{-3} M $Fe(Ph_2\ phen)_3^{3+}$; ◑ 4.0×10^{-3} M *p*-dimethoxybenzene and 4.0×10^{-3} M $Fe(Ph_2\ phen)_3^{3+}$; ◐ 2.0×10^{-4} M *p*-dimethoxybenzene and 7.8×10^{-3} M $Fe(bipy)_3^{3+}$.

The second order rate constants for the oxidation of a series of aromatic compounds with $Fe(phen)_3(pF_6)_3$ and $Fe(5\text{-}NO_2\ phen)_3(ClO_4)_3$ are listed in Table 2. The rate constants for the other Fe(III) complexes with some aromatic compounds are listed in Table 7, together with the standard reduction potentials of Fe(III) complexes.

The rates (log k) in Table 7 are linearly related to the standard reduction potentials of the Fe(III) oxidants, i.e. $\log k = -16.9\ E^0 + \text{constant}$, which is equivalent to the linear free energy relationship: $\Delta G‡ = \Delta G^0 + \text{constant}$. Thus, the activation free energy for the oxidation of aromatic compounds by the outer-sphere iron(III) complexes is directly related to the free energy change of oxidation.

Spectral titration of iron(III). The stoichiometric requirement of Fe(III) in the oxidation of the aromatic compound was determined spectrophotometrically, either by the amount of the Fe(III) consumed or the Fe(II) formed per mole of the aromatic compound [in the presence of excess Fe(III)]. The absorption spectrum of the Fe(II) formed in the reaction was the same as that of the authentic Fe(II) complex. Since the rates of oxidation of many of the substituted benzenes listed in Table 2 were slow, the two most reactive compounds (*p*-dimethoxybenzene and m-dimethoxybenzene) were chosen for the determination of the stoichiometry. The stoichiometries of the less reactive arenes were determined in trifluoroacetic acid since the reaction rates in this solvent were fast enough to allow completion within several hr. The stoichiometrics are listed in Table 8, together with those for the alkylmetals reported previously.[32]

Cyclic voltammetry. The measurement of single-sweep cyclic voltammograms (CV) of the aromatic compounds in Table 3 were described previously.[35] It is noteworthy that the CV of *p*-dimethoxybenzene was quasi-reversible, and the cathodic wave on the reverse scan was only observed at the sweep rates higher than 100 mV s^{-1}. At the sweep rate of 700 mV s^{-1}, the

Table 7. Second order rate constants for the oxidation of some aromatic compounds with a series of iron(III) complexes in CH_3CN at 25°

Iron(III) Complexes	$E^{0\,a}$	log k, (M^{-1} s^{-1})			
		1,4-$(MeO)_2$ C_6H_4	1,4-Me(MeO) C_6H_4	1,2,4,5- $Me_4C_6H_2$	1,3-$(MeO)_2$ C_6H_4
	(V)				
$Fe(5\text{-}NO_2\,phen)_3(ClO_4)_3$	1.18	2.19	-0.37	-1.06	-2.40
$Fe(5\text{-}Cl\,phen)_3(ClO_4)_3$	1.08	0.72	-2.00	-2.48	-3.89
$Fe(phen)_3(PF_6)_3$	0.98	-1.80	-3.72	-4.09	-5.46
$Fe(bpy)_3(PF_6)_3$	0.97	-1.80		-4.69	-5.34
$Fe(4,7diph\,phen)_3(ClO_4)_3$	0.91	-2.82	-4.54	-5.42	

[a]vs SCE from ref. 32 (0.24 V is subtracted from the values vs SHE).

Table 8. Stoichiometric consumption of iron(III) during the oxidation of aromatic compounds and alkylmetals

Iron(III) Complexes	Aromatic Compounds				Alkylmetals[a]	
	1,4-$(MeO)_2$ C_6H_4	1,3-$(MeO)_2$ C_6H_4	1,2,4,5- $Me_4C_6H_2$	1,2,3,4- $Me_4C_6H_2$	Me_4Pb	Et_4Pb
$Fe(5\text{-}NO_2\,phen)_3^{3+}$	2.0	2.0				
$Fe(phen)_3^{3+}$	2.1	2.4[b]	2.1[b]	2.0[b]	2.0	2.0
$Fe(4,7\text{-}diph\,phen)_3^{3+}$	2.0				2.1	2.1
$Fe(bpy)_3^{3+}$	2.0				2.0	2.0

[a]From ref. 32. [b]In CF_3CO_2H.

height of cathodic peak was comparable to the anodic current. The E^0 for *p*-dimethoxybenzene was estimated to be ~1.56 V by taking the average of the anodic and the cathodic peak potentials.

Application of Marcus theory to the oxidation of aromatic compounds and alkylmetals by outer-sphere iron(III) complexes

The second order rate constant k for outer-sphere electron transfer can be evaluated from Marcus theory[49] by using the modified expression:[42]

$$k = Z \exp\left[-\frac{\lambda}{4}\left\{1+\frac{E^0_{ox}-E^0_{red}}{2}\right\}^2\right] \quad (42)$$

where λ is the reorganization energy and $Z = 10^{11}\,M^{-1}\,s^{-1}$. The free energy change ΔG^0 is given by the oxidation and reduction potentials of the arene (or alkylmetal) and the Fe(III) oxidant, respectively, as $\Delta G^0/F = E^0_{ox} - E^0_{red}$, where F is the Faraday constant.

The line in Fig. 8 for the alkylmetals RM is drawn from the rate constants k evaluated by eqn (42), using $\lambda = 41$ kcal mol^{-1} and the values of E^0_{ox} and E^0_{red} as listed in Ref. 42. For the aromatic compounds included in Fig. 8, E^0_{ox} was taken as E_p in Table 4.[28] Unfortunately, the reorganization energies are unknown for these arenes, and λ was thus treated as an adjustable parameter in Table 9. The fit to the experimental rate constants is reasonable for λ between 30 and 40 kcal mol^{-1}. Note that the difference in the slopes for Ar and RM in Fig. 8(b) arises from the difference in the driving forces for eqns (28) and (34), respectively.

Acknowledgements—We wish to thank the National Science Foundation for financial support of this research and Dr. S. Shaik for a preprint of his paper.[46]

REFERENCES

[1a]P. Pfeiffer and T. Bottler, *Chem. Ber.* **51**, 1819 (1918); [b]P. Pfeiffer, W. Jowleff, P. Fischer, P. Monti and H. Mully, *Liebigs Ann.* **412**, 253 (1916); [c]R. Kuhn and T. Wagner-Jauregg, *Ber. Dtsch. Chem. Ges.* **63**, 2662 (1930); [d]R. Kuhn and T. Wagner-Jauregg, *Helv. Chim. Acta.* **13**, 9 (1930).

[2a]M. C. Kloetzel, *Organic Reactions*, Vol. 4, p. 9. Wiley, New York (1948); [b]R. B. Woodward, *J. Am. Chem. Soc.* **64**, 3058 (1942).

[3]L. J. Andrews and R. M. Keefer, *Ibid.* **75**, 3776 (1953).

Table 9. Second order rate constants for the oxidation of arenes with $Fe(phen)_3^{3+}$ in acetonitrile at 25°

Aromatic Compound	E_p-E^0_{red}	log k_{exp}[a]	log k_{calc}[b]	
			λ = 40	λ = 30
	(V)		(kcal mol^{-1})	(kcal mol^{-1})
$1,4\text{-}(MeO)_2C_6H_4$	0.53	-1.80	-1.50	0.10
$1,3\text{-}(MeO)C_6H_4$	0.73	-4.04	-3.81	-2.40
$1,4\text{-}MeO(Me)C_6H_4$	0.74	-3.72	-3.93	-2.53
$1,3\text{-}MeO(Me)C_6H_4$	0.83	-5.46	-5.03	-3.75
$MeOC_6H_5$	0.99	-7.70	-7.09	-6.05
$1,3,5\text{-}Me_3C_6H_3$	1.13	-8.22	-9.00	-8.20
$1,2,4,5\text{-}Me_4C_6H_2$	0.93	-4.09	-6.31	-5.17
$1,2,3,4\text{-}Me_4C_6H_2$	0.92	-4.24	-6.18	-5.03

[a]For $Fe(phen)_3^{3+}$ in Table V. [b]Calculated from eq 42.

[4a]R. S. Mulliken, *Ibid.* **74**, 811 (1952); *J. Phys. Chem.* **56**, 801 (1952); [b]R. S. Mulliken and W. B. Person, *Molecular Complexes*, A Lecture and Reprint Volume, Wiley-Interscience: New York (1969).

[5]For weak EDA complexes of the type described in this study, the charge separation in the excited state in eqn (2) is nearly, if not complete. See N. Mataga and M. Ottolenghi, *Molecular Association* (Edited by K. Hoster), Vol. 2, p. 31, refs cited therein; Academic Press, New York (1979); see also, S. Nagakura, *Excited States* (Edited by E. C. Lim), Vol. 2, p. 334. Academic Press, New York (1975).

[6]R. Foster, *Organic Charge-Transfer Complexes.* Academic Press, London (1969).

[7a]J. K. Williams, D. W. Wiley and B. C. McKusick, *J. Am. Chem. Soc.* **84**, 2210, 2216 (1962); [b]M. Sasaki, H. Tsuzuki and M. Okamoto, *J. Org. Chem.* **44**, 652 (1979); [c]J. V. Jouanne, H. Kelm and R. Huisgen, *J. Am. Chem. Soc.* **101**, 151 (1979); [d]M. Sasaki, H. Tsuzuki and J. Osugi, *J. Chem. Soc.* Perkin II 1596 (1980); [e]Y. Uosaki, M. Nakahara, M. Sasaki and J. Osugi, *Chem. Lett.* 727 (1979); [f]P. D. Bartlett, *Quart. Rev. Chem. Soc.* **24**, 473 (1970); [g]S. Nishida, *Angew. Chem.* Internat. Edit. **4**, 328 (1972); [h]F. Kataoka, S. Nishida, *Chem. Lett.* 1115 (1980); [i]R. Huisgen, and H. Graf, *J. Org. Chem.* **44**, 2594 (1979).

[8a]J. Sauer, *Angew. Chem.* Internat. Edit. **6**, 16 (1967). In this review, the involvement of the EDA complex in the Diels–Alder reaction suggested by Woodward[26] is mentioned as a still unsolved problem. [b]J. Sauer and R. Sustmann, *Angew. Chem.* Internat. Edit. **19**, 779 (1980). In this latest exhaustive review of the mechanistic aspects of the Diels–Alder reaction, no attention is paid to EDA complexes. [c]A. Wasserman, *Diels–Alder Reactions.* Elsevier, New York (1965).

[9a]R. Huisgen, *Acc. Chem. Res.* **10**, 117 (1977). In this review, the question of whether the EDA complex is an intermediate during the cycloaddition is disregarded, owing to the absence of a method which allows a decision to be made. See also ref. 9*b*, *c*. [b]R. Huisgen, *Pure & Appl. Chem.* **52**, 2283 (1980); [c]R. Huisgen, *Ibid.* **53**, 171 (1981).

[10]L. J. Andrews and R. M. Keefer, *J. Am. Chem. Soc.* **77**, 6284 (1955). The experimental rate constant, k_{exp}, is related to k_1 and k_2 in eqn (3) as: $k_{exp} = k_1K_{DA}/(1 + K_{DA}[D])$, and in eqn (4) as: $k_{exp} = k_2/(1 + K_{DA}[D])$, in the presence of excess donor. Thus, both kinetic formulations have the same concentration dependence on D.

[11a]V. D. Kiselev and J. G. Miller, *J. Am. Chem. Soc.* **97**, 4036 (1975); [b]M. Lofti, and R. M. G. Roberts, *Tetrahedron* **35**, 2123, 2131 (1979).

[12a]H. J. F. Angus and D. Bryce-Smith, *Proc. Chem. Soc.* 326 (1959); *J. Chem. Soc.* 4791 (1960); [b]G. O. Schenck and R. Steinmetz *Tetrahedron. Lett.* 1 (1960); [c]E. Grovenstein Jr., D. V. Rao and J. W. Taylor, *J. Am. Chem. Soc.* **83**, 1705 (1961).

[13a]D. Bryce-Smith and J. E. Lodge, *J. Chem. Soc.* 2675 (1962); [b]D. Bryce-Smith and A. Gilbert, *Tetrahedron* **32**, 1309 (1976); **33**, 2459 (1977); refs. cited; [c]D. Bryce-Smith, A. Gilbert and B. Halton, *J. Chem. Soc.* Perkin I 1172 (1978); [d]T. Kobayashi, *Chem. Rev.* (in Japanese) **1**, 283 (1973); [e]P. Boule, J. Roche and J. Lemaire, *J. Chim. Phys.* **74**, 593 (1977); [f]T. Mukai, K. Sato and Y. Yamashita, *J. Am. Chem. Soc.* **103**, 670 (1981); [g]M. Ohashi, S. Suwa, Y. Osawa and K. Tsujimoto, *J. Chem. Soc.* Perkin I 2219 (1979); [h]F. D. Lewis and R. J. DeVoe, *J. Org. Chem.* **45**, 948 (1980); [i]D. R. Arnold, P. C. Wong, A. J. Maroulis and T. S. Cameron, *Pure & Appl. Chem.* **52**, 2609 (1980).

[14a]J. D. Coyle, *Chem. Rev.* **78**, 97 (1978); [b]T. Wagner-Jauregg, *Synthesis* 165 (1980); [c]D. Bryce-Smith, B. Foulger, J. Forrester, A. Gilbert, B. H. Orger and H. M. Tyrrell, *J. Chem. Soc.* Perkin I 55 (1980); [d]H.-D. Scharf, H. Leismann, W. Erb, H. W. Gaidetzka and J. Aretz, *Pure & Appl. Chem.* **41**, 581 (1975); [e]A. Cox, P. de Mayo and R. W. Yip, *J. Am. Chem. Soc.* **88**, 1043 (1966).

[15]Shown by the selective excitation of the CT band. See R. Robson, P. W. Grubb and J. A. Barltrop, *J. Chem. Soc.* 2153 (1964).

[16]J. P. Simons, *Trans. Faraday Soc.* **56**, 391 (1960). The involvement of the CT excited state is not examined in this study. However, see Refs. 18 and 19*a*.

[17a]R. B. Woodward and R. Hoffmann, *The Conservation of Orbital Symmetry.* Academic Press, New York (1970); [b]The concerted [4s + 2s]-photocyclo-additions are symmetry-forbidden.

[18]N. D. Epiotis and R. L. Yates, *J. Org. Chem.* **39**, 21 (1974).

[19a]N. D. Epiotis, *Angew. Chem.* Internat. Edit. **13**, 751 (1974); [b]N. D. Epiotis, *J. Am. Chem. Soc.* **94**, 1924, 1935 (1972); [c]N. D. Epiotis and S. Shaik, *Ibid.* **100**, 1, 9 (1978); [d]N. D. Epiotis, *J. Am. Chem. Soc.* **95**, 1191, 1214 (1973).

[20]S. Fukuzumi, K. Mochida and J. K. Kochi, *J. Am. Chem. Soc.* **101**, 5961 (1979).

[21]S. Fukuzumi and J. K. Kochi, *J. Org. Chem.* **46**, 4116 (1981). See Refs. cited therein.

[22]H. A. Benesi and J. H. Hildebrand, *J. Am. Chem. Soc.* **71**, 2703 (1949); see also W. B. Person, *Ibid.* **87**, 167 (1965).

[23a]A. I. Konvalov and V. D. Kiselev, *Z. Org. Khim.* **2**, 142 (1966); [b]R. Boschi, E. Clar and W. Schmidt, *J. Chem. Phys.* **60**, 4406 (1974).

[24]H. C. Gardner and J. K. Kochi, *J. Am. Chem. Soc.* **98**, 2460 (1976).

[25]T. Okuyama, M. Nakada, K. Toyoshima and T. Fueno, *J. Org. Chem.* **43**, 4546 (1978).

[26a]J. Aihara, M. Tsuda and H. Inokuchi, *Bull. Chem. Soc. Japan* **43**, 3067 (1970); [b]Ref. 4*b* and Refs. cited.

[27]R. J. Klingler, J. K. Kochi, *J. Am. Chem. Soc.* **102**, 4790 (1980).

[28]R. J. Klingler and J. K. Kochi, *J. Phys. Chem.* **85**, 1731 (1981).

[29a]See D. D. Macdonald, *Transient Techniques in Electrochemistry.* Plenum Press: New York (1977); [b]The exception was *p*-dimethoxybenzene, as described in the Experimental.

[30a]T. Osa, A. Yildiz and T. Kuwana, *J. Am. Chem. Soc.* **91**, 3994 (1969); [b]A. Bewick, G. J. Edwards, J. M. Mellor and S. Pons, *J. Chem. Soc.*, Perkin II 1952 (1977); [c]V. D. Parker and R. N. Adam, *Tetrahedron Lett* 1721 (1969); [d]D. H. Evans, *Acc. Chem. Rsch.* **10**, 313 (1977).

[31a]cf W. H. Tamblyn, R. J. Klingler, W. S. Hwang and J. K. Kochi, *J. Am. Chem. Soc.* **103**, 3161 (1981); [b]Note that the slope in Fig. 4b for the aromatic compounds is close to unity, owing to the constancy of ΔG^a for aromatic cations. Likewise, when ΔG^a for the alkylmetal cations is included in Fig. 4(a), the slope is improved from 0.7 to ~1.1.

[32]C. L. Wong and J. K. Kochi, *J. Am. Chem. Soc.* **101**, 5593 (1979).

[33a]S. Fukuzumi and J. K. Kochi, *J. Am. Chem. Soc.* **103**, 7240 (1981); [b]The value of $Z = 10^{11}$ M^{-1} s^{-1} was used in the expression: $\Delta G‡ = -RT \ln (k/Z)$.

[34a]H. Masuhara and N. Mataga, *Bull. Chem. Soc. Japan* **45**, 43 (1972); [b]M. Ottolenghi, *Acc. Chem. Rsch.* **6**, 153 (1973); [c]T. Kobayashi, S. Matsumoto and S. Nagakura, *Chem. Lett.* 235 (1974). See also Ref. [5].

[35a]See Ref. [21], [b]Since the heats of formation of these EDA complexes are uniformly small, there is essentially no difference in the energetics of reaction 28 derived either from the separated arene and TCNE or from the EDA complex, as the precursor.

[36]K. Egawa, N. Nakashima, N. Mataga and C. Yamanaka, *Chem. Phys. Lett.* **8**, 108 (1971); *Bull. Chem. Soc. Japan* **44**, 3287 (1971).

[37]See M. Lofti and R. M. G. Roberts, *Tetrahedron* **35**, 2137 (1979). The free energy of solution of neutral arenes has been evaluated to be only 1 ~ 2 kcal mol^{-1} from solubility measurements in CH_2Cl_2 and CCl_4.

[38a]T. Kobayashi and S. Nagakura, *Bull. Chem. Soc. Japan* **47**, 2563 (1974); [b]H. Bock and W. Kaim, *Chem. Ber* **111**, 3552 (1978); [c]G. M. Anderson, III, P. A. Kollman, L. N. Domelsmith and K. N. Houk, *J. Am. Chem. Soc.* **101**, 2344 (1979).

[39a]M. E. Peover, *Electroanal. Chem.* **2**, 1 (1967); [b]B. Case, *Reactions of Molecules at Electrodes* (Edited N. S. Hush), p. 125. Wiley-Interscience, New York (1971).

[40a]R. C. Larson, R. T. Iwamoto and R. N. Adams, *Anal. Chim. Acta* **25**, 371 (1961); [b]The value of C for the $Ag/AgClO_4$ ref in MeCN is 4.70 V, which is decreased by 0.30 V when related to the SCE ref.

[41a]See S. Fukuzumi and J. K. Kochi, *J. Am. Chem. Soc.* **102**, 2141 (1980), and Ref. [20] for a further discussion of this point. [b]See also Ref. [21].

[42]S. Fukuzumi, C. L. Wong and J. K. Kochi, *J. Am. Chem. Soc.* **102**, 2928 (1980) for a distinction between inner-sphere and outer-sphere electron transfer mechanisms.

[43a]G. Dulz and N. Sutin, *Inorg. Chem.* **2**, 917 (1963); [b]H. Diebler and N. Sutin, *J. Phys. Chem.* **68**, 174 (1964); [c]K. W. Hicks and J. R. Sutter, *Ibid.* **75**, 1107 (1971) and Ref. [32] for leading Refs.

[44]For treatments based on perturbation theory, see [a]K. Fukui, *Fortschr. Chem. Forsch.* **15**, 1 (1970); *Acc. Chem. Rsch.* **4**, 57 (1971); in *Chemical Reactivity and Reaction Paths* (Edited by J. Klopman), Wiley-Interscience, New York (1974); [b]I. Fleming, *Frontier Orbitals and Organic Chemical Reactions*, Wiley, New York (1976); [c]K. N. Houk, *Acc. Chem. Rsch.* **8**, 361 (1975); [d]E. Heilbronner and H. Bock, *Das HOMO-Model und Seine Anwendung*, Verlag Chemie (1970).

[45]The polar type as defined by Epiotis[19] corresponds to the normal and inverse types of Diels–Alder reaction, as described by Sauer[8] and Sustmann. [R. Sustmann, *Pure Appl. Chem.* **40**, 569 (1974).]

[46]S. Shaik, *J. Am. Chem. Soc.* **103**, 3692 (1981).

[47]According to Shaik,[46] the bond pair in Scheme 4 consists of the two odd electrons which are spin paired, and prepared for bonding as the "*image*" of the product.

[48]C. L. Wong, K. Mochida, A. Gin, M. A. Weiner and J. K. Kochi, *J. Org. Chem.* **44**, 3979 (1979).

[49]See the Marcus treatment in the Experimental. [a]R. J. Marcus, *J. Chem. Phys.* **24**, 966 (1956); **26**, 867 (1957); *Discuss. Faraday Soc.* **29**, 21 (1960); [b]N. Sutin, *Inorganic Biochemistry* (Edited by G. L. Eichhorn), Vol. 2, p. 611. Elsevier, Amsterdam (1973); [c]W. L. Reynolds and R. W. Lumry, *Mechanisms of Electron Transfer*. Ronald Press, New York (1966).

[50a]V. D. Parker and O. Hammond, *Acta. Chemica Scandinavia* **B31**, 883 (1977); [b]O. Hammerich and V. D. Parker, *J. Am. Chem. Soc.* **96**, 4289 (1974); [c]B. S. Jensen and V. D. Parker, *Ibid.* **97**, 5211 (1975).